Effects of ocean acidification on the dissolution rates of reef-coral skeletons

Ocean acidification threatens the foundation of tropical coral reefs. This study investigated three aspects of ocean acidification: (i) the rates at which perforate and imperforate coral-colony skeletons passively dissolve when pH is 7.8, which is predicted to occur globally by 2100, (ii) the rates of passive dissolution of corals with respect to coral-colony surface areas, and (iii) the comparative rates of a vertical reef-growth model, incorporating passive dissolution rates, and predicted sea-level rise. By 2100, when the ocean pH is expected to be 7.8, perforate *Montipora* coral skeletons will lose on average 15 kg $CaCO_3$ m^{-2} $year^{-1}$, which is approximately – 10.5 mm of vertical reduction of reef framework per year. This rate of passive dissolution is higher than the average rate of reef growth over the last several millennia and suggests that reefs composed of perforate *Montipora* coral skeletons will have trouble keeping up with sea-level rise under ocean acidification. Reefs composed of primarily imperforate coral skeletons will not likely dissolve as rapidly, but our model shows they will also have trouble keeping up with sea-level rise by 2050.

Effects of ocean acidification on the dissolution rates of reef-coral skeletons

Robert van Woesik*[1], Kelly van Woesik[2], Liana van Woesik[2], Sandra van Woesik[2]

[1]Florida Institute of Technology

150 W. University Blvd., Melbourne FL, 32901 USA

ph: +1 321 674 7475; Fax: +1 321 674 7238

[2] Melbourne, Florida, USA

* Correspondence to: rvw@fit.edu

Key Words: Corals, dissolution, acidification, reef growth, climate change.

12 # Abstract

13 Ocean acidification threatens the foundation of tropical coral reefs. This study investigated three
14 aspects of ocean acidification: (i) the rates at which perforate and imperforate coral-colony
15 skeletons passively dissolve when pH is 7.8, which is predicted to occur globally by 2100, (ii) the
16 rates of passive dissolution of corals with respect to coral-colony surface areas, and (iii) the
17 comparative rates of a vertical reef-growth model, incorporating passive dissolution rates, and
18 predicted sea-level rise. By 2100, when the ocean pH is expected to be 7.8, perforate *Montipora*
19 coral skeletons will lose on average 15 kg $CaCO_3$ m^{-2} $year^{-1}$, which is approximately – 10.5 mm
20 of vertical reduction of reef framework per year. This rate of passive dissolution is higher than the
21 average rate of reef growth over the last several millennia and suggests that reefs composed of
22 perforate *Montipora* coral skeletons will have trouble keeping up with sea-level rise under ocean
23 acidification. Reefs composed of primarily imperforate coral skeletons will not likely dissolve as
24 rapidly, but our model shows they will also have trouble keeping up with sea-level rise by 2050.

Introduction

Ocean acidification

As humans continue to burn fossil fuels at an unprecedented rate, the concentration of carbon dioxide (CO_2) in the atmosphere is presently higher than it has been for the last 420,000 years (Petit et al. 1999; Hansen et al. 2006; Hoegh-Guldberg et al. 2007). The oceans uptake a large proportion of the atmospheric CO_2, increasing the concentrations of both carbonic acid and bicarbonate ions, and reducing the concentration of carbonate ions, shifting the ocean's acid-base balance toward a lower pH (Broeker 1983; Caldeira and Wickett 2003; Silverman et al. 2009). The increase in ocean acidification directly threatens calcifying marine organisms, such as reef-building corals and the myriad of species that rely on corals for protection and sustenance (Hoegh-Guldberg et al. 2007; Rodolfo-Metalpa et al. 2011).

The oceanic pH has already decreased by 0.1 pH units since the 18th century, and is expected to drop by another 0.2 – 0.4 pH units by 2100. Yet the oceans are not homogenous in regard to rates of reductions in carbonate ions. Although warm waters increase reaction rates, thermodynamic principles and Henry's Law tells us that cool temperate and polar waters absorb asymmetrically more CO_2 than tropical waters, and are therefore closer to unity than the more super-saturated tropical waters (Broecker 1983). Yet the tropical oceans are changing at a more rapid rate and are acidifying more quickly than the cooler waters most likely because of the relationship of rapidly increasing ocean temperature and reaction rates (Zeebe et al. 2008). Moreover, the Pacific Ocean is more acidic than the Atlantic Ocean, and shoaling saturation depth is around 500 m in the Pacific and 4500 m in the Atlantic (Feely et al. 2004; Millero 2007).

There is increasing evidence that ocean acidification, through the increase in the partial pressure of carbon dioxide (pCO_2) and the subsequent changes in the concentration of carbonate and bicarbonate ions, reduces rates of coral calcification, which are directly proportional to the saturation state of aragonite in the shallow oceans (Langdon and Atkinson 2005). Other studies have shown that calcification rates are proportional to the concentration of carbonate ions in the water column (Anthony et al. 2008; Marubini et al. 2008). These studies are essentially synonymous, however, because the aragonite and calcite saturation state (Ω) is the product of the concentrations of calcium and carbonate ions divided by an equilibrium constant. Since the salt concentration, including calcium ions, stemming from terrestrial weathering hasn't changed in the oceans for over 1.5 billion years, the aragonite saturation state is essentially a measure of carbonate ions in the oceans.

Perhaps more importantly is the strong interaction effects between temperature and ocean acidification on coral calcification rates (Reynaud et al. 2003; Erez et al. 2010). Indeed, the optimal window of physiological performance of a given marine species at a given temperature will be narrowed under acidification (Portner 2010). Calcification of corals under ambient temperature do not necessarily change with increased pCO_2, but calcification decreases when both temperature and pCO_2 are elevated (Reynaud et al. 2003). Yet several studies have shown that many corals are unaffected by external carbonate ion concentrations because they have the capacity to up-regulate internal pH by actively exchanging internal hydrogen ions for calcium ions through Ca-ATPase transportation (Al-Horani et al. 2003; Allemand 2004; McCulloch et al. 2012). By modifying their internal chemistry, live corals may buffer themselves from ocean acidification. Coral skeletons, however, have no internal-buffering capacity because they are not

protected by coral membranes (Rodolfo-Metalpa et al. 2011; Ries 2011). Coral skeletons are instead subjected to the raw and immediate threats of ocean acidification and will be subjected to dissolution when the ocean's pH declines.

Accretion of coral reefs

The accretion of coral reefs occurs over geological time periods when rates of calcium carbonate ($CaCO_3$) production exceed rates of destruction and dissolution (Neumann and MacIntyre 1985; Buddemeier and Hopley 1988; Glynn 1997; Perry et al. 2013). The interaction between production and destruction depends on the consistency of coral cover through time. For example, where coral cover is consistently low, reef accretion is minimal (Neumann and MacIntyre 1985). Most modern reefs, however, support little more than 28% live coral cover (Bruno and Selig 2007), and are essentially veneers over pre-existing, antecedent foundations of $CaCO_3$ (Adey 1978; Hopley 1982). For example, the Florida Keys only supported, on average, 2-3% of live coral cover in 2011 (Office of National Marine Sanctuaries 2011). Therefore, reefs with high carbonate cover and few live corals are particularly vulnerable to ocean acidification.

The average modern, shallow seaward coral reef in the Indo-Pacific, with high coral cover, has been estimated to produce about 4 kilograms of calcium carbonate per square meter of reef per year, which equates with an upward reef-growth rate of approximately 3 mm per year (Smith and Kinsey 1976). These estimates were based on alkalinity reduction techniques subjected to a pH of 8.2, equivalent to the pH of today's oceans. By 2100 the ocean's pH is expected to be 7.8, and we hypothesize that the destructive processes associated with ocean acidification might outweigh the constructive processes. The rates of dissolution of reef framework may however also depend on

flow rates, the extent of cementation of reef framework, and on the porosity of corals and their surface area.

Reef cementation and coral porosity

Reefs vary in porosity depending on both: (i) the local rates of sedimentation and the extent to which those sediments become consolidated, or lithified, within the reef framework, and (ii) the extent of cementation of the reef framework. Both processes depend in part on exposure to water-flow rates (MacIntyre and Marshall 1988). High-energy, windward reefs consistently exposed to large waves are generally more highly cemented than low-wave energy, leeward reefs because mass-transfer rates influence rates of cementation. Cementation involves the infilling of intra-skeletal pores with either Mg calcite or aragonite (MacIntyre and Marshall 1988). While the extent of cementation affects the dislodgment of reef substrate and the tenacity of corals to remain attached to reefs during storms (Madin et al. 2012), the extent of reef cementation may also affect dissolution rates during ocean acidification because the infilling of pores by cements decreases the surface area of exposure (Cubillas et al. 2005).

Reef corals also vary in porosity (Gladfelter 1982; Hughes 1987). Although all modern corals secrete orthorhombic aragonite fusiform crystals, as small as 1-3 μm (Gladfelter 1982), corals vary considerably in the arrangement of the crystals, which influences the internal surface area that is exposed (Fig. 1). Fast-growing corals, such as *Montipora* and *Acropora*, are mostly perforate corals (Gladfelter 1982), whereas slow-growing corals, such as *Pectinia* and *Symphyllia*, are imperforate (Table 1). An extreme example of imperforate skeletons is evident by the observation of occasional floating, massive *Symphyllia* colonies (DeVantier 1992). Because of the fused nature of the dissepiments and their imperforate skeletons, gases are trapped in the

111 septal chambers and upon dislodgement from reefs, for example during a storm, the colonies will
112 float. Perforate corals however, do not have the capacity to isolate septal chambers.

113 The internal porosity of coral skeletons, at the scale of 0.5—1 mm (Fig. 1), increases the
114 available surface area of chemical exchange and therefore increases the potential rates of
115 dissolution. Walter and Morse (1984) showed that rates of dissolution of skeletal carbonates were
116 inversely related to grain-size diameter and surface roughness, with fine grained carbonates
117 dissolving faster than large, rough surfaces. However, we should not discount the possibility that
118 perforate and imperforate corals also differ in other aspects, beyond the obvious differences in
119 porosity, and therefore we question whether surface area is a useful predictor of rates of passive
120 dissolution of both perforate and imperforate corals.

121 This study will examine whether the porosity and the surface area of coral skeletons will
122 influence their rate of dissolution when the ocean pH is 7.8, which is predicted to occur by 2100.
123 More specifically, we tested three hypotheses: (1) that perforate *Montipora* coral skeletons are
124 more likely to passively dissolve than imperforate *Pectinia* coral skeletons at a pH of 7.8, (2) that
125 the rates of passive dissolution of coral-colony skeletons are proportional to their surface areas,
126 and (3) future reef accretion rates under ocean acidification will differ depending on the nature of
127 the coral assemblages, with perforate coral assemblages unable to keep up with predicted sea-
128 level rise and imperforate coral assemblages faring a better chance at keeping up with sea-level
129 rise and ocean acidification.

Materials and Methods

Acidification experiments

In order to test the first hypothesis, perforate *Montipora* colonies (Figure 1) and imperforate *Pectinia* colonies without tissue (Figure 2) were used to make comparisons of weight loss when immersed in seawater and held in zero-flow conditions (i.e., to test passive dissolution), and held at a pH of 8.2, equivalent to the pH of today's oceans, and compared with colonies held at a pH of 7.8, which is predicted to occur globally by 2100. Fifteen skeletal samples (≤5 cm) of *Montipora* spp. colonies and fifteen skeletal samples of *Pectinia* spp. were collected from the fringing reefs of Okinawa, Japan in 2001. In order to test the second hypothesis, we used a variety of growth forms of *Montipora*, including submassive, branching, encrusting, and foliose. Colonies of *Pectinia* with different surface areas were used for experimental treatments, but all samples were foliose because *Pectinia* is only found as foliose colonies on modern coral reefs.

Before pH treatments, the samples were placed in a drying oven at 40ºC for 48 h and weighed (g) using a Sartorius Research Balance. Each treatment sample was then placed in a separate container of seawater that was maintained at a pH of 7.8 by adding diluted acetic acid to match the predicted pH of the seawater in the year 2100 (Intergovernmental Panel on Climate Change [IPCC], 2007). The control samples were placed in seawater that was maintained at a pH of 8.2, to match modern ocean conditions, and maintained at 24ºC and a salinity of 35. Total alkalinity was not measured in this study. Seawater was changed every 2 days. After 7 days the samples were rinsed and dried in a drying oven at 40°C for 48 hours, and re-weighed. The volume of each coral sample (mL) was calculated using a displacement method and the surface area of each coral sample (cm^2) was calculated using a single wax-dipping method (Veal et al. 2010).

Data analyses

The difference in dry weight (g) before and after the acid treatment was calculated for each coral sample. To correct for differences in initial weight, the loss of calcium carbonate was divided by each coral's initial weight. To compare differences in dissolution rates that may have varied in accordance with growth form, we undertook an analysis of variance (ANOVA) and a Tukey's post-hoc test using R (R Development Core Team, 2012). The relationship between the surface area, volume, and the loss of calcium carbonate was examined using curve fitting with Matlab®.

Accretion-dissolution model

The loss of calcium carbonate was extrapolated from the change in calcium carbonate per gram cm^{-2} day^{-1}, to the equivalent loss of calcium carbonate per kg m^{-2} y^{-1}. This loss was compared with the geological literature and converted to the approximate equivalent of vertical reduction of reef framework in mm per year (Smith and Kinsey 1976). The loss was compared with predicted sea-level rise (Vermeer and Rahmstorf 2009). In order to achieve this goal, the reef accretion rates were modeled as an ordinary differential equation:

$$dA/dt = (a.A)/A + b.S - (c.D)/A \quad (1),$$

where A is the accretion of a reef relative to time (t); a is the accretion coefficient determined by coral and coralline algal growth minus the bioerosion rates (input as 7 mm per year for reefs that accrete the maximum of 10 kg $CaCO_3$ m^{-2} y^{-1}; 3 mm per year for reefs that accrete 4 kg $CaCO_3$ m^{-2} y^{-1}; and 0.75 mm per year for reefs that accrete 1 kg $CaCO_3$ m^{-2} y^{-1}, with a 50% average reef porosity, after Kinsey 1979 and Smith 1983); b is a coefficient for sedimentation (S), input as 1

mm per year for consistency; and *c* is a coefficient for the dissolution (D) rates. The equations were solved using Runge-Kutta methods using the ode45 solver in Matlab® (code is available in the appendix).

The results of passive dissolution were input into our reef-growth model and compared with projections of global sea-level rise, from 1990 to 2100 following Vermeer and Rahmstorf (2009), which did not consider regional isostatic rebound effects, regional tectonics, and local land-use effects. The sea-level rise projections used different IPCC (2007) emission scenarios, including the B1 scenario representing a +1.8ºC global increase in temperature, the A2 scenario representing a +3.4ºC global increase in temperature, and the A1F1 scenario representing a 4ºC global increase in temperature.

Results

There was a significant difference ($p < 0.0258$) in coral skeleton weight loss that was dependent on coral colony porosity (Figure 3). The skeletons of foliose, perforate *Montipora* coral colonies passively dissolved significantly (post-hoc Tukey test, $p < 0.011$) faster than the skeletons of foliose, imperforate *Pectinia* coral colonies (Figure 3). The skeletons of foliose *Montipora* corals also lost more calcium carbonate than other *Montipora* growth forms (Figure 3). Foliose *Montipora* corals also lost more calcium carbonate than other *Montipora* growth forms (Figure 3). There was a strong negative relationship between the surface area of *Montipora* corals and the loss of calcium carbonate, suggesting that the larger the surface area of *Montipora* colonies the more rapidly the corals dissolved (Figure 4). The rate of calcium carbonate loss followed the equation, $CaCO_3$ loss = $- 0.005 \times \exp^{0.017 * \text{surface area}}$. The loss of $CaCO_3$ of perforate *Montipora* was

193 approximately 0.000042 g $CaCO_3$ cm^{-2} day^{-1} (- 0.42 g $CaCO_3$ m^{-2} d^{-1}, or - 15.3 kg $CaCO_3$ m^{-2} y^{-1}).
194 This loss in calcium carbonate is approximately equivalent to – 10.5 mm of vertical reduction of
195 reef framework per year.

196 In contrast, the skeletons of imperforate *Pectinia* colonies showed no consistent (passive)
197 dissolution at a pH of 7.8, suggesting that the loss of weight in low pH treatments was no
198 different than the weight loss in controls (Figures 3 and 5). There was no significant relationship
199 between the surface area of *Pectinia* coral colonies and their rate of passive dissolution (Figure
200 5). There was also no significant relationship between dissolution rates and the volume of either
201 *Montipora* or *Pectinia* colonies.

202 *Accretion-dissolution model*

203 The sea-level rise projections from 1990 to 2100 were constructed using different IPCC (IPCC
204 2007) emission scenarios, including the B1 scenario, representing a +1.8°C global increase in
205 temperature, the A2 scenario representing a +3.4°C global increase in temperature, and the A1F1
206 scenario representing a 4°C global increase in temperature (Figure 6; Vermeer and Rahmstorf,
207 2009). These sea-level projections were compared with three different reef-building capacities in
208 conjunction with rates of perforate and imperforate coral skeletons (equation 1) under ocean
209 acidification (Figures 6 and 7). The model with high dissolution rates, which included perforate
210 skeletons, and consistently high coral cover (10 kg $CaCO_3$ m^{-2} y^{-1}) are not expected to keep up
211 with sea level rise under ocean acidification (Figure 6). By contrast, the model with low
212 dissolution rates, which included imperforate corals, could continue to grow reefs and keep up
213 with sea level rise, but only reefs consistently supporting high coral cover (10 kg $CaCO_3$ m^{-2} y^{-1})

and only to 2050. Around 2050, the model shows that the rates of sea level rise are expected to increase faster than the rates at which corals can grow reefs (Figure 7).

Discussion

This study examined whether the destructive processes involving the dissolution of calcium carbonate might over-ride the accretionary potential of coral reefs when the oceans pH drops to 7.8, which is predicted to occur by 2100. We examined the rates of skeletal dissolution of two Indo-Pacific corals, *Montipora* and *Pectinia*, subjected to a pH of 7.8. Rates of passive dissolution were directly proportional to the surface area of corals, but only for the perforate *Montipora*; dissolution was less predictable for the imperforate *Pectinia*. The average loss of *Montipora* $CaCO_3$ per surface area was 15.3 kg m^{-2} y^{-1}, which was 3 times more than the average growth rates of modern reefs (4 kg $CaCO_3$ m^{-2} y^{-1}) (Smith 1983; Smith and Kinsey 1976; Kinsey 1979).

We should however, treat the comparative results between skeletal dissolution and reef growth, with caution even though the units match ($CaCO_3$ m^{-2} y^{-1}). In the comparison above, our data were extrapolated across at least five orders of magnitude spatially, from grams per cm^2 to kilograms per m^2, and at least six orders of magnitude temporally, from skeletal dissolution over weeks to reef growth over millennia. Yet our results, on the passive dissolution rates of porous *Montipora* coral skeletons (- 0.42 g $CaCO_3$ m^{-2} d^{-1}) and the recent field results from Cyronak et al. (2013), on the passive dissolution rates of carbonate sediments on Heron Island (Great Barrier

Reef, Australia), are the same. Cyronak et al. (2013) also showed that adding flow to experiments more than doubled dissolution rates because of advection processes.

We also note that Smith, Kinsey, and co-workers, originally calculated calcium carbonate production using advection alkalinity reduction techniques that measured change in alkalinity across reef flats over minutes. The maximum rate of modern reef growth has been estimated at 9.6 kg $CaCO_3$ m^{-2} yr^{-1} on a back-reef of Johnston Atoll (16°N, 169°W), that supported "heavy" coral cover (but the percentage coral cover was not provided in the original publication) (Kinsey 1979). Other estimates using X-radiographs and extrapolation techniques showed similar results, ranging from 9 kg $CaCO_3$ m^{-2} y^{-1} for reefs in the Caribbean with uncharacteristically high coral cover (38%) (Stearn et al. 1977), to less than 1 kg $CaCO_3$ m^{-2} y^{-1} for reefs with low coral cover (Dullo 2005).

Although our results show rapid rates of *Montipora* dissolution, modern-reef framework is not all *Montipora*. Rates of carbonate dissolution will also depend on the type of coral assemblages that are present on reefs and their densities. Globally, approximately 404 coral species are perforate, and 432 are imperforate (Table 1), yet most Indo-Pacific reefs are dominated by *Acropora, Montipora, Porites*, and faviids; and Caribbean reefs are dominated by *Porites*, *Siderastrea*, and *Orbicella*. Therefore, most modern reefs are primarily supporting perforate corals, and these corals have disproportionately contributed to vertical reef accretion through the Holocene (Veron 1995, Wood 1999).

Still, changing the pH of seawater is only one of the changes that will occur to reefs subjected to climate change. Sea level will also rise with increasing global temperature (Smith and

Buddemeier 1992; Vermeer and Rahmstorf 2009). The conservative estimates of sea-level rise from the IPCC (2007), which did not consider ice-sheet dynamics, showed that sea level will increase 20-60 cm by 2100 (approximately 4 mm a year). More recent estimates of sea level rise by Vermeer and Rahmstorf (2009) predict a sea level increase of 75-90 cm by 2100, which is approximately 9 mm a year. Our predictive model, although extrapolating across several spatial and temporal scales, showed that coral reefs composed of perforate skeletons and supporting few live corals, will have trouble keeping up with sea level rise under ocean acidification. These results, although tentative, suggest that more quantitative studies are necessary to determine the potential of reefs to keep up with sea level rise by hierarchically quantifying the production versus dissolution rates of reefs in relation to: (i) coral cover, (ii) coral-community composition, (iii) habitat type, and (iv) the regional oceanography.

Acknowledgments

Our special thanks extend to Richard Turner, Biological Sciences Department, College of Science, Florida Institute of Technology, for the use of his laboratory equipment and to Gayle Duncan for preparing the scanning electron microscope images. The corals were collected at (26º21'34.47"N, 127º44'20.96"E) with a permit to Robert van Woesik from the Okinawan prefectural government, Japan.

References

Adey W.H. (1987) Coral reef morphogenesis: A multi-dimensional model, Science 202: 831-837

Al-Horani F.A., Al-Moghrabi S.M., de Beer D. (2003) The mechanism of calcification and its relation to photosynthesis and respiration in the scleractinian coral *Galaxea fascicularis*, Marine Biology 142: 419-426

Allemand D., Ferrier-Pagès C., Furla P., Houlbrèque F., Puverel S., Reynaud S., Tambutté E., Tambutté S., Zoccola D. (2004) Biomineralisation in reef-building corals: from molecular mechanisms to environmental control, Comptes Rendus Palevol 3: 453–467

Anthony K.R.N., Kline D.I., Diaz-Pulido G., Dove S., Hoegh-Guldberg O. (2008) Ocean acidification causes bleaching and productivity loss in coral reef builders, Proceedings of the National Academy of Science 105: 17442–17446

Broecker W.S (1983) The Ocean, Scientific American 249: 146-48

Bruno J.F., Selig E.R (2007) Regional decline of coral cover in the Indo-Pacific: timing, extent, and subregional comparisons, PLoS ONE, 2, 8, e711. doi:10.1371/journal.pone.0000711

Buddemeier R.W., Hopley D (1988) Turn-ons and turn offs: Causes and mechanisms of the initiation and termination of coral reef growth, Proceedings of the 6th International Coral Reef Symposium, Townsville, Australia, 8-12 August 1988, 1988, 1, 253-261

Caldera K., Wickett M.E. (2003) Anthropogenic carbon and ocean pH, Nature 425: 365

Cubillas P, Kohler S, Prieto M, Chairat C, Oelkers EH (2005) Experimental determination of the dissolution rates of calcite, aragonite, and bivalves. Chemical Geology 216: 59-77

Cyronak T, Santos IR, Eyre BD (2013) Permeable coral reef sediment dissolution driven by elevated *p*CO2 and pore water advection. Geophysical Research Letters 40:1-6

DeVantier L.M (1992) Rafting of tropical marine organisms on buoyant coralla, Mar. Ecol. Prog. Ser. 86, 301-302

Dullo W.C. (2005) Coral growth and reef growth: a brief review, Facies 51: 33-48

Erez J, Reynaud S, Silverman J, Schneider K, Allemand D (2010) Coral calcification under ocean acidification and global change. In, Editors, Z. Dubinsky & N Stambler, Coral reefs: an ecosystem in transition, Springer, New York, 551 pp

Feely RA, Christopher L. Sabine CL, Lee K, Will Berelson W, Kleypas J, Fabry VJ, Frank J. Millero FJ (2004) Impact of Anthropogenic CO_2 on the $CaCO_3$ System in the Oceans. S*cience 305:* 362–366

Fine M., Tchernov D (2007) Scleractinian coral species survive and recover from decalcification, Science 315: 1811

Gladfelter EH (1982) Skeletal development in *Acropora cervicornis:*I. patterns of calcium carbonate accretion in the axial corallite. Coral Reefs 1:45-51

Glynn P.W (1997) Bioerosion and coral-reef growth: a dynamic balance, In Birkeland, C. (Ed.), Life and Death of coral reefs, Chapman & Hall, 68-95

Hansen L., Sato M., Ruedy R., Lo K., Lea D.W., Medina-Elizade M. (2006) Global temperature change, PNAS 103: 14288-14293

Hoegh-Guldberg O., Mumby P., Hooten A.J., Steneck R.S., Greenfield P., Gomez E., Harvell C.D., Sale P.F., Edward A.J., Caldiera K., Knowlton N., Eakin C.M., Iglesias-Prieto R., Muthiga N., Bradbury R.H., Dubi A., Hatziolos M.E (2007) Coral reefs under rapid climate change and ocean acidification, Science 318: 1737-1742

Hautmann M (2004) Effect of End-Triassic CO_2 maximum on carbonate sedimentation and marine mass extinction. Facies 50:257–261

Hopley D (1982) The geomorphology of the Great Barrier Reef: Quaternary development of coral reefs, John Wiley-Interscience, New York, pp 453

Hughes TP (1987) Skeletal density and growth form of corals. Marine Ecology Progress Series 35: 259-266

Intergovernmental Panel on Climate Change (IPCC 2007), Climate Change 2007: the physical science basis, Contribution of Working Group 1 to the Fourth Assessment Report of the Intergovernmental Panel on Climate Change, Cambridge Univ. Press, Cambridge, p 793

Kinsey D.W (1979) Carbon turnover and accumulation by coral reefs, PhD Dissertation thesis, University of Hawaii, 284

Kroeker K.J., Kordas R.L., Crim R.N., Singh G.G (2010) Meta-analysis reveals negative yet variable effects of ocean acidification on marine organisms, Ecology Letters 13: 1419–1434

Langdon C., Atkinson M.J (2005) Effect of elevated pCO_2 on photosynthesis and calcification of corals and interactions with seasonal change in temperature/irradiance and nutrient enrichment, J. Geophys. Res.110, C09S07, doi:10.1029/2004JC002576

MacIntyre I., Marshall J.F (1988) Submarine lithification in coral reefs: same facts and misconceptions, Proc 6th Int. Coral Reef Symp., Australia, 1, 263-272

Madin JS, Hughes TP, Connolly SR (2012) Calcification, storm damage, and population resilience of tabular corals under climate change. PLOS ONE 10.1371/journal.pone.0046637

Manzello D.P., Kleypas J.A., Budd D.A., Eakin C.M., Glynn P.W., Langdon C. (2008) Proceedings of the National Academy of Sciences 105: 10450-10455

Marubini F., Ferrier-Pages C., Furla P., Allemand D (2008) Coral calcification responds to seawater acidification: a working hypothesis towards a physiological mechanism, Coral Reefs 7: 491–499

McCulloch M., Falter J., Trotter J., Montagna P (2012) Coral resilience to ocean acidification and global warming through pH up-regulation, Nature Climate Change, 2012, doi: 10.1038/NCLIMATE1473

Millero FJ (2007). The marine inorganic carbon cycle. Chem. Rev. 2007, 107, 308-341

Morse JW, Arvidson, RS, Luttge A (2007) Calcium Carbonate Formation and Dissolution. Chem. Rev. 107: 342-381

Neumann A.C., MacIntyre I (1985) Reef response to sea level rise: keep-up, catch-up or give-up, Proc. 5th International Coral Reef Congress, 3: 105-110

Office of National Marine Sanctuaries, Florida Keys National Marine Sanctuary Condition Report 2011, U.S. Department of Commerce, National Oceanic and Atmospheric Administration, Office of National Marine Sanctuaries, Silver Spring, MD, 2011, 105

Perry CT, Murphy GN, Kench PS, Smithers SG, Edinger EN, Steneck RS, Mumby PJ (2013). Caribbean-wide decline in carbonate production threatens coral reef growth. Nature Communications 4:1402. doi:10.1038/ncomms2409

Petit JR, Jouzel J, Raynaud D, Barkov NI, Barnola J.-M, Basile I, Bender M, Chappellaz J, Davis M, Delaygue G, Delmotte M, Kotlyakov VM, Legrand M, Lipenkov VY, Lorius C, Pepin L, Ritz C, Saltzman E, Stievenard M (1999) Climate and atmosphere history of the past 420,000 years from the Vostok ice core, Antartica. Nature 399: 429-436[2]

Portner H.-O (2010) Oxygen- and capacity-limitation of thermal tolerance: a matrix for integrating climate-related stressor effects in marine ecosystems. J Exp Biol 213:881-893

Reynaud S, Leclercq N, Romaine-Lioud S, Ferrier-Pagès C, Jaubert J, Gattuso J-P (2003) Interacting effects of CO_2 partial pressure and temperature on photosynthesis and calcification in a scleractinian coral. Glob Change Biol 9:1660–1668

Ries J. (2011) Acid ocean cover up, Nature Climate Change 1: 294-295

Rodolfo-Metalpa R., Houlbrèque F., Tambutté E., Boisson F., Baggini C., Patti F.P., Jeffree R., Fine M., Foggo A., Gattuso J.P., Hall-Spencer J.M. (2011) Coral and mollusc resistance to ocean acidification adversely affected by warming, Nature Climate Change, doi: 10.1038/NCLIMATE1200

R Development Core Team (2012). R: A language and environment for statistical computing. R Foundation for Statistical Computing, Vienna, Austria. ISBN 3-900051-07-0, URL http://www.R-project.org.

Silvermann J., Lazor B., Cao L., Caldiera K., Erez J. (2009) Coral reefs may start dissolving when atmospheric CO_2 doubles, Geophysical Research Letters 36: L05606, doi:10.1029/2008GL036282

373 Smith S.V. (1983) Coral reef calcification, In Barnes, D.G. (Ed.), Perspectives on coral reefs,
374 Brian Clouston Publisher, 240-247
375 Smith S.V., Kinsey D.W. (1976) Calcium carbonate production, coral reef growth, and sea level
376 change, Science 194, 937-939

377 Smith S.V., Buddemeier R.W. (1992) Global change and coral reef ecosystems, Annual Review
378 of Ecology and Systematics 23: 89-118

379 Stearn C.W., Scoffin T.P., Martindale W. (1977) Calcium carbonate budget of a fringing reef on
380 the west coast of Barbados, Bull. Marine Science 27: 479-510

381 Veal C.J., Carmi M., Fine M. (2010) Increasing the accuracy of surface area estimation using
382 single wax dipping of coral fragments. Coral Reefs 29: 893-897

383 Vermeer M., Rahmstorf S. (2009) Global sea level linked to global temperature, Proceedings of
384 the National Academy of Sciences 106, 21527-21532

385 Veron JEN (1995) Corals in space and time: the biogeography and evolution of the Scleractinia.
386 University of New South Wales Press, Sydney, pp 321

387 Veron JEN (2008) Mass extinctions and ocean acidification: biological constraints on geological
388 dilemmas. *Coral Reefs* 27: 459-472

389 Walter L.M., Morse J.W. (1984) Reactive surface area of skeletal carbonates during dissolution:
390 effect of grain size, J. of Sedimentary Petrology 54: 1081-1090

391 Wood R (1999) Reef evolution. Oxford University Press, Oxford, pp 414

392 Zeebe RE, JC Zachos, Caldira K, Tyrrell T (2008) Carbon emissions and acidification. Science
393 321: 51-52

Figure captions

Figure 1. *Montipora*. Scanning electron microscope image of *Montipora* skeleton*;* scale bar is 500 micrometer.

Figure 2. *Pectinia.* Scanning electron microscope image of *Pectinia* skeleton*;* scale bar is 500 micrometer.

Figure 3. Comparative loss of calcium carbonate. Loss of calcium carbonate, divided by the initial weight (g), of four different coral growth forms of *Montipora* coral skeletons, and one growth form of *Pectinia* coral skeleton, when exposed to pH 7.8 seawater for 7 days. The graph also depicts the controls for *Montipora* and *Pectinia* coral skeletons, which were exposed to present-day seawater, at a pH of 8.2, for 7 days. The dashes are the data points, the horizontal lines on each 'bean' show the means, and each 'bean' shape follows the general the distribution of the data relative to density (constructed using the package 'beanplot' in R).

Figure 4. *Montipora* dissolution. The relationship between the surface area of the *Montipora* coral skeletons (cm^2) and the loss of calcium carbonate ($CaCO_3$) (g) over 7 days follows the equation loss = $-0.005 \times exp^{0.017 * \text{surface area}}$. The dots are the data points, the thick, black line represents the equation, and the dotted lines represent the 95% confidence intervals.

Figure 5. *Pectinia* dissolution. The relationship between the surface area of the *Pectinia* coral skeletons (cm^2) and the loss of calcium carbonate ($CaCO_3$) (g) over 7 days.

Figure 6. Accretion potential of perforate corals and predicted sea-level rise. The projections of expected rates of coral-reef accretion relative to rates of dissolution of reefs composed of mainly perforate corals, with 3 different densities of corals (low, medium and high modeled as 1, 4, and 10 kg $CaCO_3$ m^{-2} y^{-1}), along with projections of global sea-level rise (not considering regional isostatic rebound effects, regional tectonics, and local land-use effects) and potential reef-accretion rates from 1990 to 2100 following Vermeer and Rahmstorf (2009) for different IPCC (2007) emission scenarios, where the B1 scenario is green and represents a +1.8ºC global increase in temperature; the A2 scenario is blue and represents a +3.4ºC global increase in temperature; the A1F1 scenario is red and represents a 4ºC global increase in temperature**.**

Figure 7. Accretion potential of imperforate corals and predicted sea-level rise. The projections of expected rates of coral-reef accretion relative to rates of dissolution of reefs composed of mainly imperforate corals, with 3 different densities of corals (low, medium and high modeled as 1, 4, and 10 kg $CaCO_3$ m^{-2} y^{-1}), along with projections of global sea-level rise (as in Figure 6).

425 **Table 1.** Porosity of scleractinian corals. Scleractinian coral families, the number of species in
426 each family, and the general porosity of the coral skeletons. Classifications were based on the
427 porosity of the colony walls, the coenosteum, and the collumellae at the scale of 1 mm^2. There are
428 approximately 404 perforate species and 432 imperforate coral species, globally.

Table 1(on next page)

Porosity of scleractinian corals.

Scleractinian coral families, the number of species in each family, and the general porosity of the coral skeletons. Classifications were based on the porosity of the colony walls, the coenosteum, and the collumellae at the scale of 1 mm^2. There are approximately 404 perforate species and 432 imperforate coral species, globally.

Family	Number of species	Porosity
Acroporidae	271	Perforate
Agariciidae	45	Imperforate
Astrocoeniidae	15	Imperforate
Caryophylliidae	7	Imperforate
Dendrophylliidae	19	Imperforate
Euphyllidae	17	Imperforate
Faviidae	130	Imperforate
Fungiidae	46	Imperforate
Meandrinidae	12	Imperforate
Merulinidae	12	Imperforate
Mussidae	52	Imperforate
Oculinidae	16	Imperforate
Pectiniidae	29	Imperforate
Pocilloporidae	31	Imperforate
Poritidae	101	Perforate
Siderastreidae	32	Perforate
Trachphylliidae	1	Imperforate

Figure 1

Figure 1. *Montipora*.

Scanning electron microscope image of *Montipora* skeleton; scale bar is 500 micrometer.

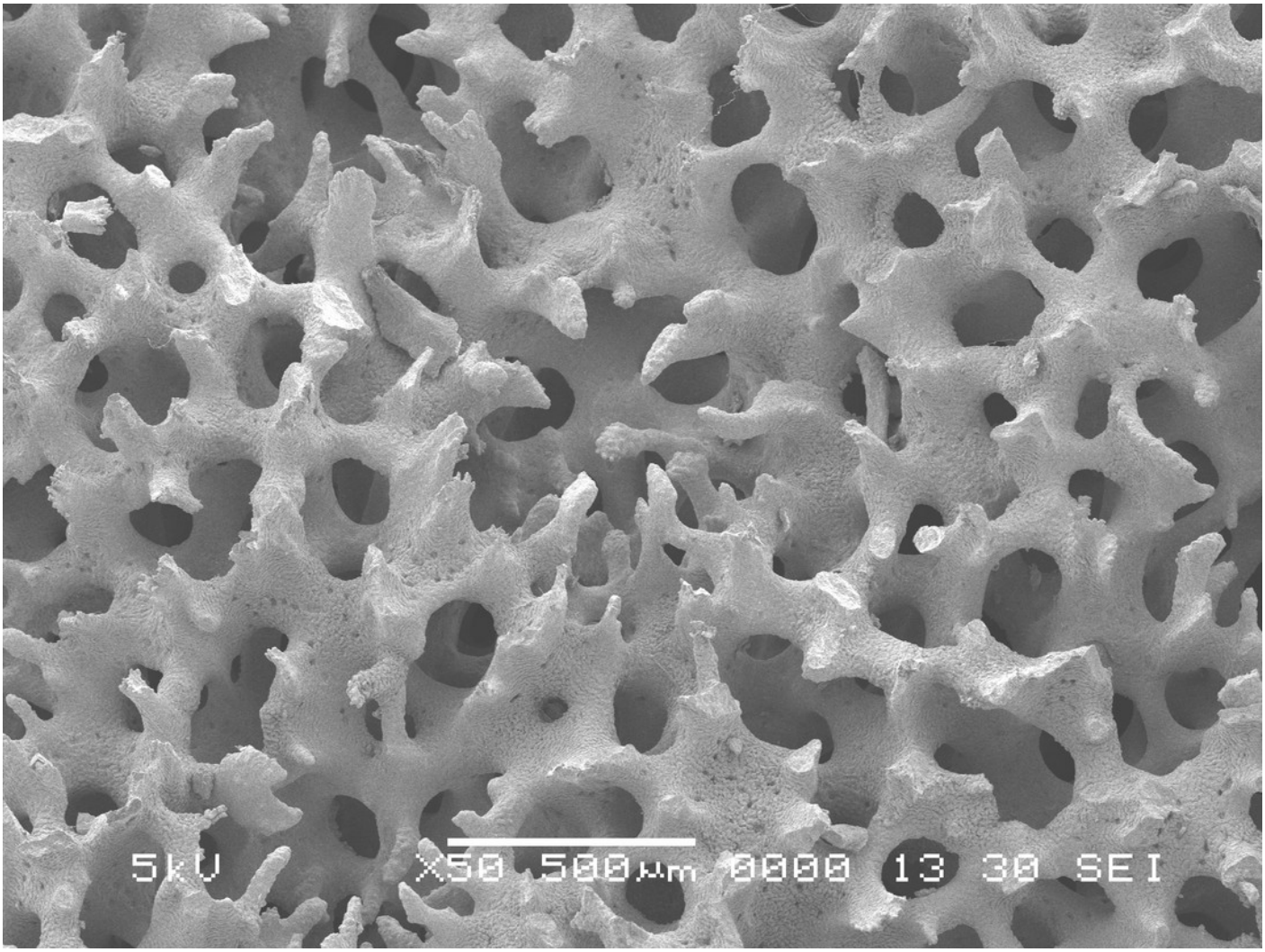

Figure 2

Figure 2. *Pectinia*.

Scanning electron microscope image of *Pectinia* skeleton; scale bar is 500 micrometer.

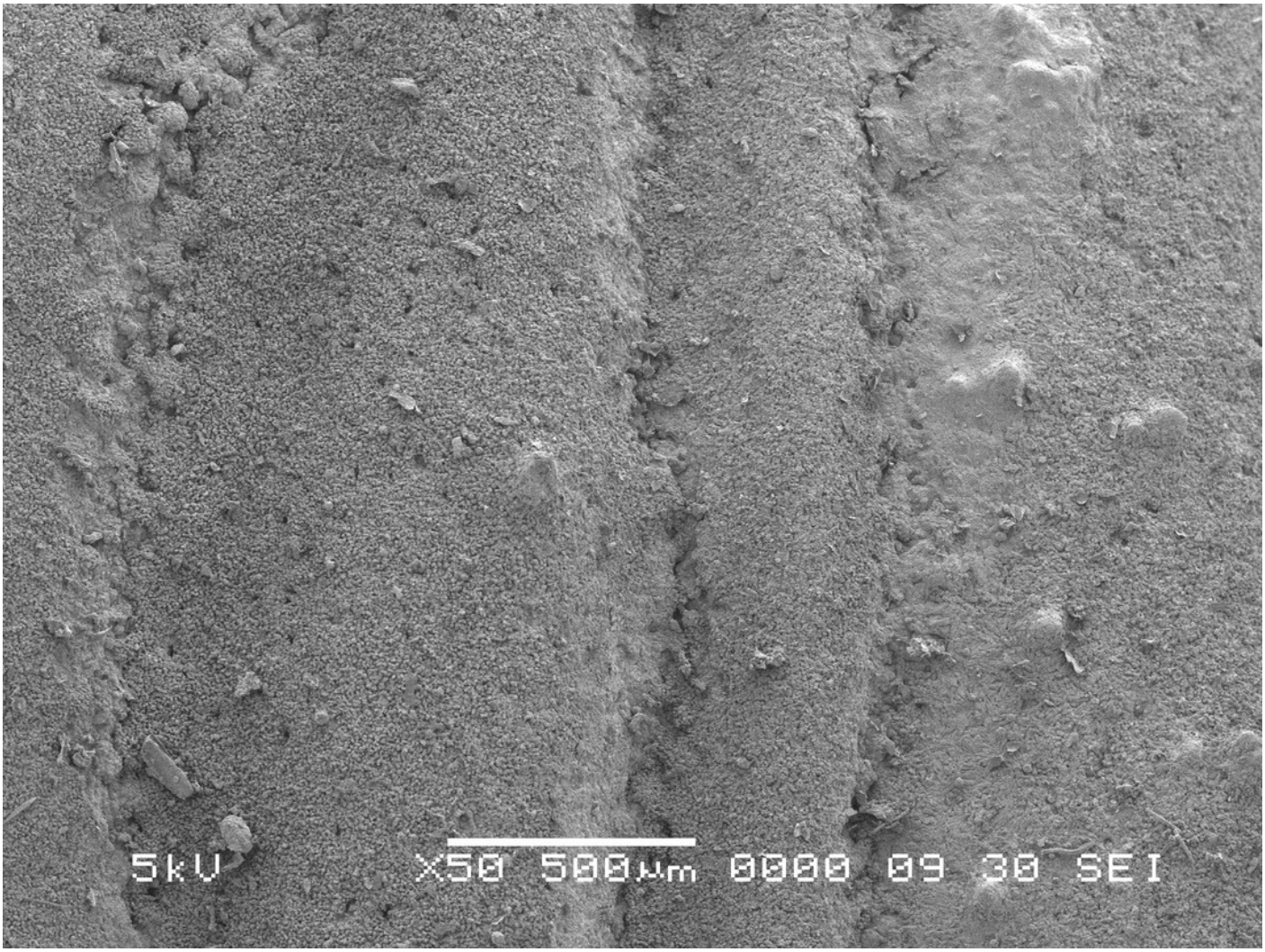

Figure 3

Figure 3. Comparative loss of calcium carbonate.

Loss of calcium carbonate, divided by the initial weight (g), of four different coral growth forms of *Montipora* coral skeletons, and one growth form of *Pectinia* coral skeleton, when exposed to pH 7.8 seawater for 7 days. The graph also depicts the controls for *Montipora* and *Pectinia* coral skeletons, which were exposed to present-day seawater, at a pH of 8.2, for 7 days. The dashes are the data points, the horizontal lines on each ‘bean’ show the means, and each ‘bean’ shape follows the general the distribution of the data relative to density (constructed using the package 'beanplot' in R).

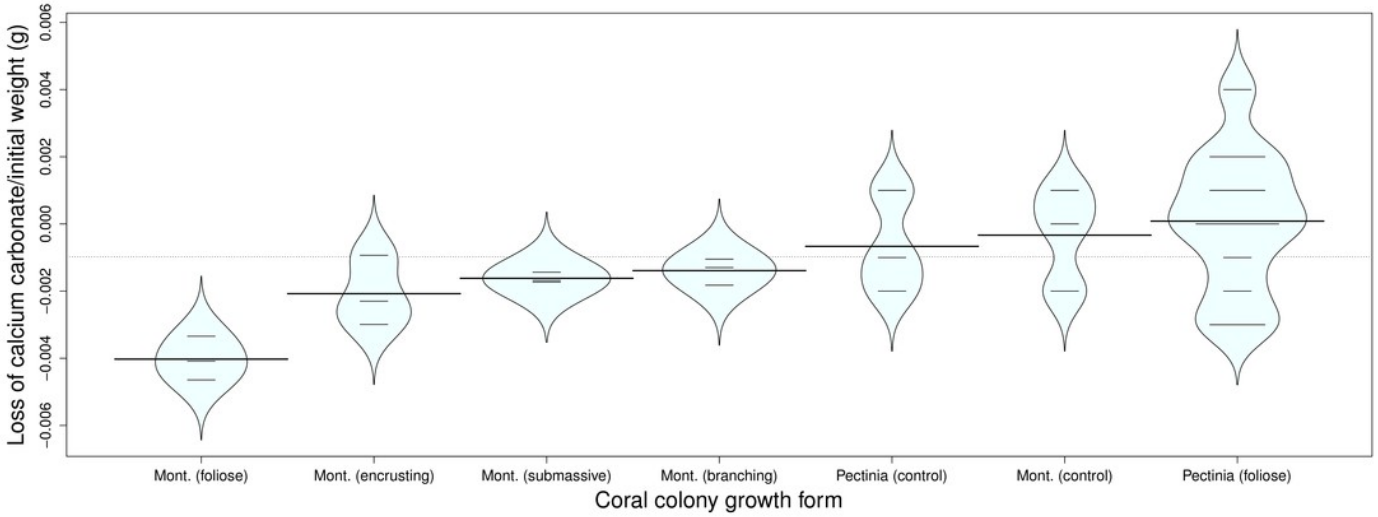

Figure 4

Figure 4. *Montipora* dissolution.

The relationship between the surface area of the *Montipora* coral skeletons (cm^2) and the loss of calcium carbonate ($CaCO_3$) (g) over 7 days follows the equation loss = - 0.005 x exp ^{0} ^{017} * surface area. The dots are the data points, the thick, black line represents the equation, and the dotted lines represent the 95% confidence intervals.

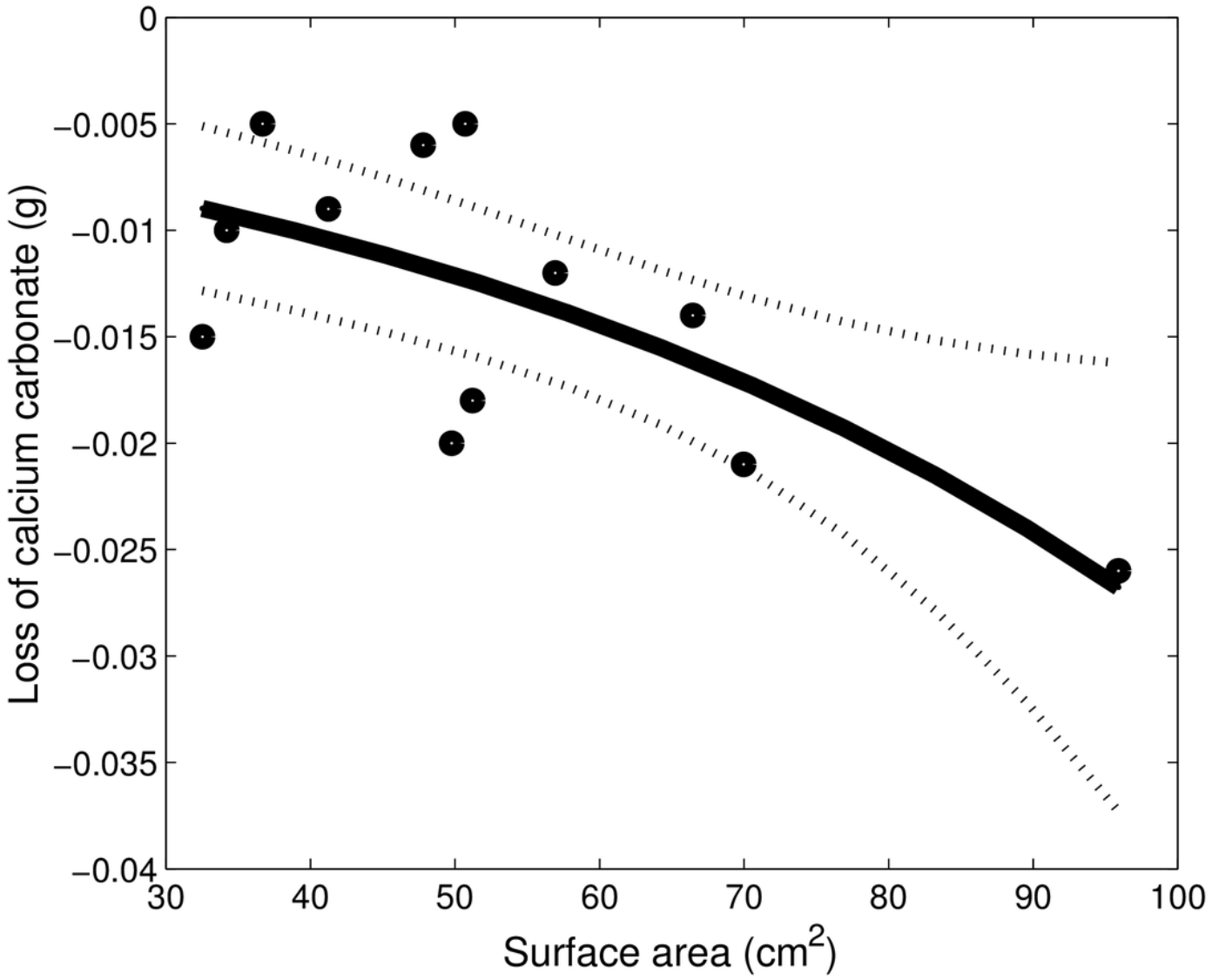

Figure 5

Figure 5. *Pectinia* dissolution.

The relationship between the surface area of the *Pectinia* coral skeletons (cm^2) and the loss of calcium carbonate ($CaCO_3$) (g) over 7 days.

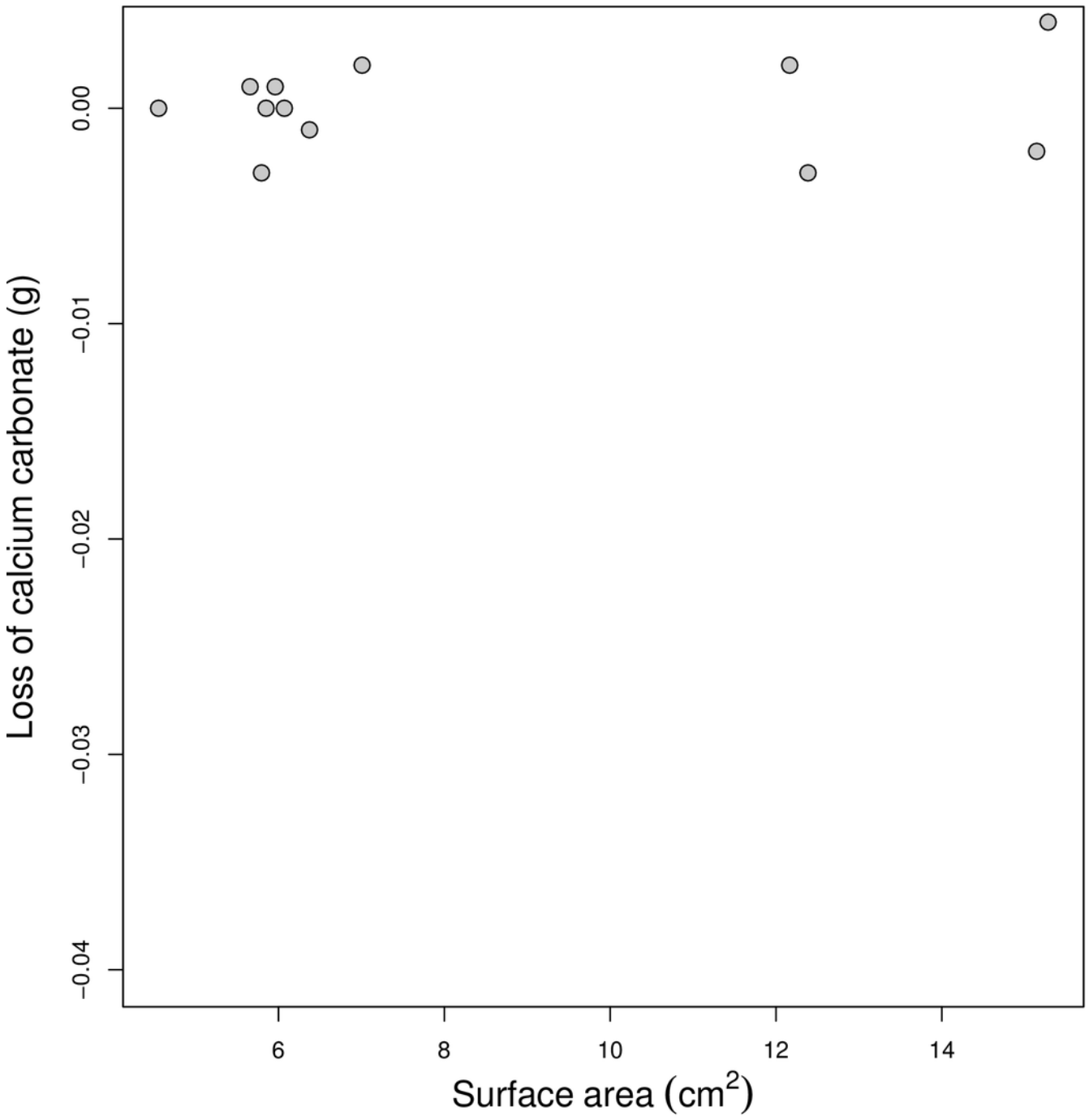

Figure 6

Accretion potential of perforate corals and predicted sea-level rise.

The projections of expected rates of coral-reef accretion relative to rates of dissolution of reefs composed of mainly perforate corals, with 3 different densities of corals (low, medium and high modeled as 1, 4, and 10 kg $CaCO_3$ m^{-2} y^{-1}), along with projections of global sea-level rise (not considering regional isostatic rebound effects, regional tectonics, and local land-use effects) and potential reef-accretion rates from 1990 to 2100 following Vermeer and Rahmstorf (2009) for different IPCC (2007) emission scenarios, where the B1 scenario is green and represents a +1.8ºC global increase in temperature; the A2 scenario is blue and represents a +3.4ºC global increase in temperature; the A1F1 scenario is red and represents a 4oC global increase in temperature.

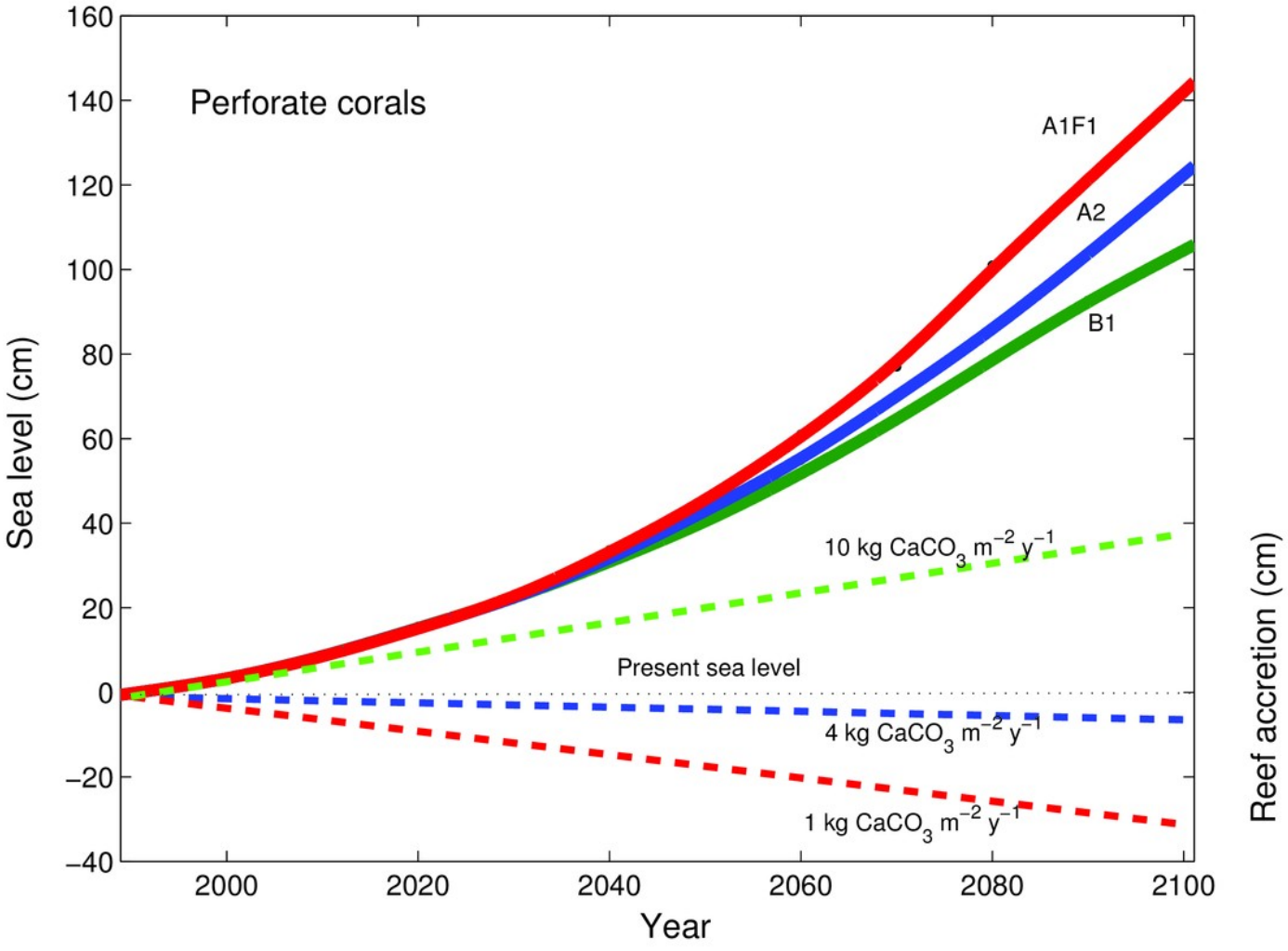

Figure 7

Accretion potential of imperforate corals and predicted sea-level rise.

The projections of expected rates of coral-reef accretion relative to rates of dissolution of reefs composed of mainly imperforate corals, with 3 different densities of corals (low, medium and high modeled as 1, 4, and 10 kg $CaCO_3$ m^{-2} y^{-1}), along with projections of global sea-level rise (as in Figure 6).